Hindawi
Geofluids
Volume 2022, Article ID 1583013, 19 pages
https://doi.org/10.1155/2022/1583013

Research Article

Seismic Response and Economic Study of New Light Steel-Wood-Plastic Structure in Rural Yunnan, China

Shujiang Jiang,[1] **Jie Yang**,[2] **Dewen Liu**,[1] **Jingran Xu**,[1] **Zhiang Li**,[1] **Liang Gao**,[1] **Yutong Yang**,[1] **and Bingxing Ma**[1]

[1]*College of Civil Engineering, Southwest Forestry University, Kunming 650000, China*
[2]*College of Engineering and Technology, The Open University of Sichuan, Chengdu 610031, China*

Correspondence should be addressed to Dewen Liu; civil_liudewen@sina.com

Received 10 March 2022; Accepted 24 May 2022; Published 24 June 2022

Academic Editor: Yue Niu

A new type of light steel-wood-plastic residential structure in rural has popular in recent years in rural Yunnan, China. The application of light steel, wood, and new plastic materials in practical engineering is gradually increasing due to its advantages of green ecology and waste utilization, and its response characteristics under earthquakes have attracted great attention. In this paper, seismic-resistant models, seismic-isolated models, and seismic-damped models for multistorey light steel-wood-plastic structures were established using the SAP2000 finite element software based on different seismic response methods. The seismic-isolated model is divided into five schemes, namely, LRB400, LRB500, LRB600, high damped, and friction pendulum-isolated bearings, and the seismic-damped model is divided into three schemes, namely, ordinary bracing, soft-steel bracing, and BRB bracing at the same locations around the 2nd floor of the building. Nonlinear time analysis was carried out for the nine schemes, comparing the period, structural interstorey displacement, base shear, top displacement, top acceleration, and economy of the structure under the action of an 8-degree earthquake. Results show that the period of the seismic-isolated system increased by approximately 130% compared to the seismic-resistant system, and the period of the damped system decreased slightly compared to the seismic system, the interstorey displacement, base shear, and top acceleration of both the seismic-isolated system and the damped system were smaller than those of the seismic-resistant system, and the seismic-isolated system decreased by approximately 40% compared to the damped system, and the seismic-isolated system was more effective than the damped system. From the comparison of postearthquake damage cost and full-cycle cost, the economic performance of the seismic-isolated structure is better than that of the damped and seismic-resistant structures. The conclusions of this paper can provide a scientific reference for promoting the use of new light steel-wood-plastic residential buildings.

1. Introduction

A new type of light steel-wood-plastic residential structure in rural Yunnan Province of China has been gradually popular in recent years. Its underlying part is traditional steel structure, and the above part is light steel structure. The wood-plastic material attached to the surface of light steel mainly plays a protective and decorative role. Light steel structure [1] is lighter than traditional steel structure generally refers to the thickness of the steel structure is not more than 10 mm, with advantages of low-carbon environmental protection, short construction period, low cost, and good seismic performance. Wood-plastic composite [2] is a high-performance composite material made of waste wood, crop straw, and other powder and plastic as raw materials. The application of light steel-wood-plastic structure [3] system in practical engineering is gradually increasing. Liu [4] discussed the advantages of low-rise cold-formed thin-wall steel structural members from the aspects of calculation method, seismic performance, and construction according to the natural disasters that occurred in China in recent years. Zhu [5] compared the two systems, traditional residential structures and cold-formed thin-walled steel structures, and concluded that the

development of cold-formed steel-walled steel structural systems in China should be accelerated and can be widely applied to the vast rural areas.

Conventional seismic resistance relies on the ductility and plasticity of the structure itself to dissipate seismic energy. From the current development, the traditional seismic resistance can no longer meet the seismic requirements of the structure. In recent years, scholars have proposed building seismic isolated and damped techniques to control the energy input to the building structure and reduce the seismic response of the structure, greatly increasing the safety of the structure.

Many researchers have made achievements in seismic isolation of light steel structures. Li et al. [6] describe the sources, characteristics, and future trends of traditional energy sources and their impact on the environment. Cao [7] studied the overall seismic performance of the system using simulated seismic shaking table tests for light steel keel houses. The main findings of Pan et al. [8] are as follows: basic design procedures are becoming standardised, mainly involving the determination of design seismic forces, selection of ground vibrations, modelling, and time analysis and performance criteria, and the use of multiple nonlinear time analyses of ground vibrations is a feature of the design of seismic isolation and energy dissipation structures. Wu et al. [9] studied the failure characteristics of different geological structures under high stress. Ma et al. [10] carried out precracking blast vibration damping tests to investigate the vibration damping effect of the precrack formed; Zhou et al. [11, 12] explored the future trends of seismic resistance, isolation, passive, and active control technologies; Zhu et al. [13] illustrated the scope, advantages, and disadvantages of the use of different seismic isolation bearings and dampers in building structures, as well as the practicality and economy of further improving seismic isolation bearings and damping devices; Zhou [14] illustrated the effectiveness of the laminated seismic-isolated system in controlling seismic response; Yuan et al. [15, 16] analysed the dynamic response of several seismic isolation structures and traditional masonry structures and concluded that the seismic isolation structure can effectively absorb seismic energy, among which the composite isolation system has the best seismic isolation effect; Wang et al. [12, 17–20] studied the variation of stresses and strains with time in structures subjected to strong dynamic loads such as explosions and impacts. Li et al. [21, 22] studied the stress-strain relationship of soil under repeated loads to provide data support for practical engineering. Natale et al. [23, 24] studied a PBEE-based method to quantify the payback time (PBT) of seismic retrofit solutions for existing RC buildings, based on the fact that the high installation costs of foundation isolation limit its widespread use in common designs; Li [25] applied different dampers to an engineering example for performance analysis; Wang [26] used three different support systems for a dynamic time analysis of the Songhua Bridge and concluded that the system equipped with dampers was more favourable for seismic resistance; Li and Zhou et al. [27, 28] introduced the composition and performance of friction pendulum and how to mitigate the seismic effect of building structures in engineering practice; Nakamura and Okada et al. [29] verified the effectiveness of seismic isolation and

Figure 1: Light steel-wood-plastic structure building.

reaction control methods by shaking table tests and seismic response analysis for three types of rubber bearings and three types of damping devices; Natale et al. and Di Sarno et al. [23, 30] studied how highly damped rubber bearings mitigate the seismic effects of steel buildings in actual earthquakes; Shahbazi and Moaddab [31] illustrated the intrinsic relationship and the acceleration and displacement response spectra of displacement-dependent dissipators in structures, as well as the principles and practical applications of displacement-dependent dissipators; Dong et al. [32, 33] studied the hysteretic force-deformation response of large dampers. Wen et al. [34] research found that unsoaked rocks are the strongest. Kong et al. [35, 36] analysed the different waveform characteristics of the structure at different periods of deformation damage to predict the development trend and pattern of the structure during damage deformation. Based on the basic characteristics and influencing factors of rock bursts and rock materials in engineering, He et al. [37, 38] introduced a new prediction index system and proposed corresponding control strategies.

Most of the above studies are focused on light steel structures, while there are few studies on new light steel-wood-plastic structures in Yunnan villages. Based on this, this paper uses the SAP2000 software to establish seismic resistance, isolated, and damped models for light steel-wood-plastic structures and conducts nonlinear analysis under earthquakes. The evolution characteristics of the seismic, isolated, and damped models of light steel-wood-plastic structure are compared and analysed. In addition, the economic benefits of different structures are compared with the whole cycle cost of the building, which provides theoretical analysis support for engineering application.

2. Project Overview and Modelling

The house (Figure 1) is located in Xishuangbanna, Yunnan Province. It is a light steel, wood, and plastic house with a total construction area of 172.2 m^2 and a height of 8 m. It has 2 floors, each with a height of 2.8 m. The house is designed to last 50 years. The design value of seismic acceleration is 0.30 g. The damping ratio under multiple earthquakes is 0.04. The basic wind pressure coefficient is 0.4 kN/m^2. The foundation is an independent foundation under a column, and the bottom steel column is rigidly connected to the

Table 1: The component materials of the light steel-wood-plastic residential structure.

Components	Cross-sectional dimensions (mm)	Material grade	Capacity (kN.m^{-3})
1st floor Frame columns	□200 × 6	Q345	78.50
1st floor Frame beams	HN200 × 100 × 4.5 × 7	Q345	78.50
2nd floor column and beams	[140 × 40 × 1.2]	Q345	78.50
Floorboards	100 mm thick reinforced concrete	C30 (HRB335)	25.00
Wood plastic panels	20 mm thick	/	13.72

foundation. The materials for each part of the building structure for this project are shown in Table 1 below.

The load values are divided into horizontal and vertical loads. The horizontal loads in the structure design are mainly seismic and wind loads, the total height of the structure is 8.0 m, and the basic combination of seismic effects and other load effects of the structural members is calculated. The constant floor load caused by the building surface is taken as 2.0 kN/m^2, the live load on the floor is taken as 2.0 kN/m^2, and the live load on the unoccupied roof is taken as 0.5 kN/m^2.

A finite element calculation model for the seismic-resistant structure, seismic isolated, and damped structure of the light steel-wood-plastic structure (shown in Figure 2) was established. The seismic-isolated models were simulated at the base position using LRB400, LRB500, LRB600, high damped, and friction pendulum isolation bearings (shown in green in Figure 2(b)). The damped model was simulated using normal bracing, soft-steel bracing, and BRB (buckling restrained brace) bracing at the same locations around the 2nd storey of the building, respectively, as indicated by the red part of Figure 2(c). The Q345 steel nonlinear materials are adopted with kinematic hysteretic type, as shown in Figure 3.

3. Seismic Wave Selection

At least two natural seismic waves and one artificial seismic wave were used for the simulation analysis. The duration of each wave should be greater than or equal to 5 times the basic natural vibration period of the building structure, and not less than 15 s. The time interval of each wave is usually 0.01 s or 0.02 s.

The predominant period of the seismic wave should selected to be as consistent as possible with the characteristic period of the site, so EL-Centro wave, Lanzhou wave, and Shanghai artificial wave were selected for analysis in this paper; these seismic waves meet with Xishuangbanna site. The seismic wave information is shown in Table 2 and illustrated in Figure 4.

4. Analysis of Elastic-Plastic Results

4.1. Analysis of Results under Seismic Action

4.1.1. Comparison of the Periods of the Seismic-Resistant Model and Seismic-Isolated Models. The modal analysis was carried out separately for the seismic-resistant model and seismic-isolated models, resulting in the following self-oscillation periods for both the light steel-wood-plastic structure with isolated bearings and the seismic-resistant model as shown in Figure 5.

It can be seen from Figure 5 that the self-oscillation period in the seismic isolation system is LRB400>LRB600>friction pendulum>highly damped≈LRB500>seismic structure in the time range of 2 to 4 s. The self-oscillation period of the light steel-wood-plastic seismic-resistant model is about 2.4 s, while the self-oscillation period of the seismic-isolated models with different types of bearings is about 5.4 s. The natural vibration period increases by about 130% compared to the seismic-resistant model. Thus, it can be seen that the basic cycle of light steel, wood, and plastic construction has been greatly extended. With the extension of the period, the self-excitation period of the building is far away from the characteristic period of the site, which effectively controls the resonance of the structure during earthquakes.

4.1.2. Comparison of Seismic Resistant and Damped Structural Cycles. The light steel-wood-plastic structure incorporates three different types of vibration damping bracing at the second level, and modal analysis of these three braces yielded a table of the first three vibration periods as shown in Figure 6. The self-oscillation periods are all normal bracing<BRB bracing<soft-steel bracing<seismic-resistant model.

4.1.3. Comparison of Structural Interstorey Displacements. The results of Figure 7 show that the interlayer displacement of light steel-wood-plastic structure under the action of Lanzhou wave has the following relations: high damping< friction pendulum<LRB500<LRB400<LRB600<normal bracing<soft-steel bracing<BRB bracing<seismic-resistant model; accordingly, the results of the action of El-Centro wave are as follows: LRB500<LRB400<LRB600<friction pendulum<high damping<normal bracing<soft-steel bracing<BRB bracing<seismic-resistant model; accordingly, the results of Shanghai artificial wave are as follows: LRB500< LRB400<LRB600<friction pendulum≈high damping<soft-steel bracing≈BRB bracing<normal bracing<seismic-resistant model. It can be concluded that the interstorey displacements produced by the seismic-resistant model are the largest; the interstorey displacements of the superstructure of the seismic isolation and seismic damping system are substantially reduced compared to those of the seismic-resistant

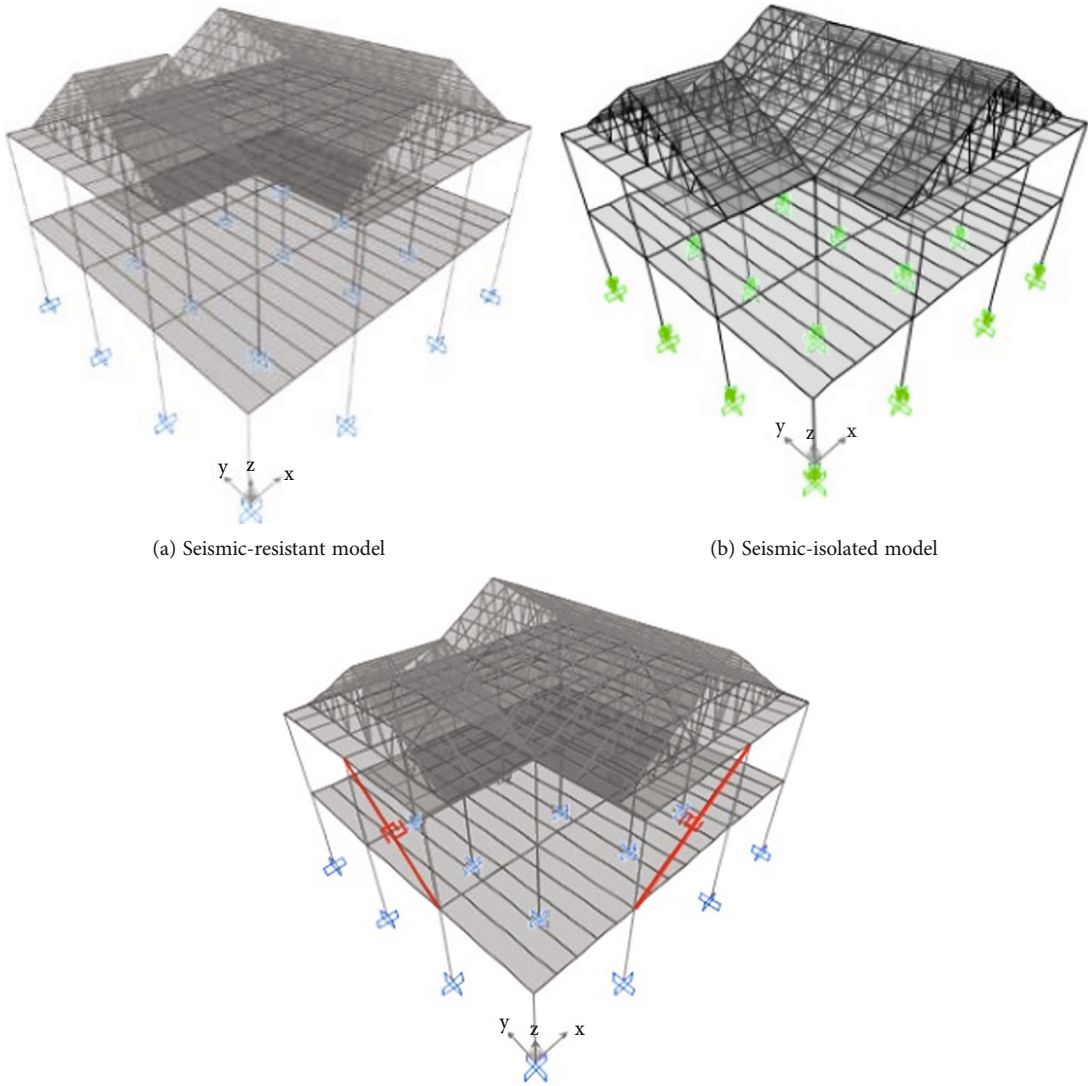

(a) Seismic-resistant model

(b) Seismic-isolated model

(c) Seismic-damped model

Figure 2: Light steel-wood-plastic structure model.

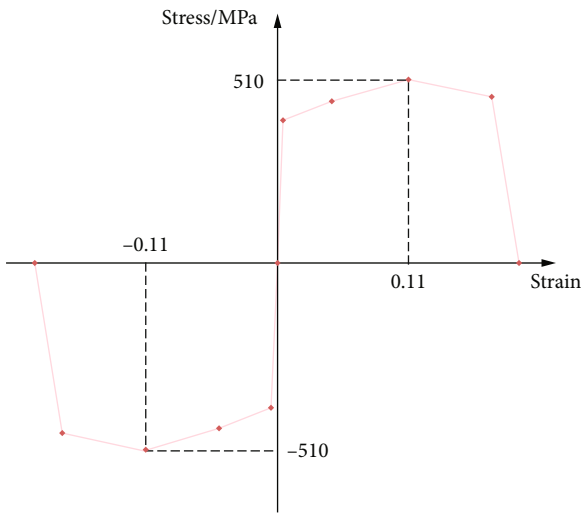

Figure 3: Structural nonlinear constitutive relation.

Table 2: Selected seismic wave record.

Seismic wave	Acceleration peak cm/s^2	Duration/ s	Time interval/s
EL-Centro	341.7	30	0.02
Shanghai artificial wave	1181.3	24.9	0.02
Lanzhou wave	196.2	30	0.02

system; the interstorey displacements produced by all five options of the seismic-isolated system are smaller than those produced by the three options of the seismic-damped models.

The lateral displacement of the top floor of the structure reflects the lateral stiffness of the building; the greater the lateral stiffness of the structure, the smaller the corresponding top floor displacement is. According to the time course

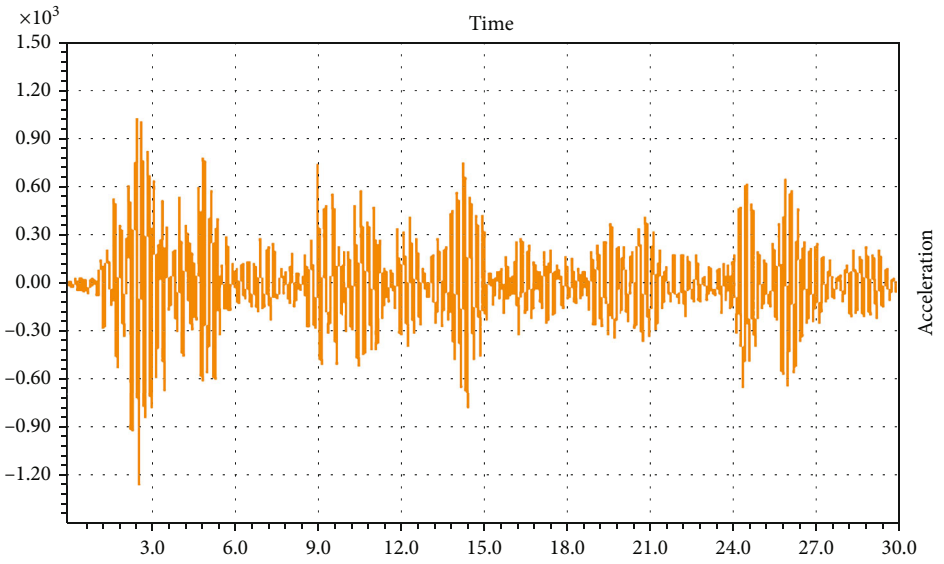

(a) EL-Centro seismic wave

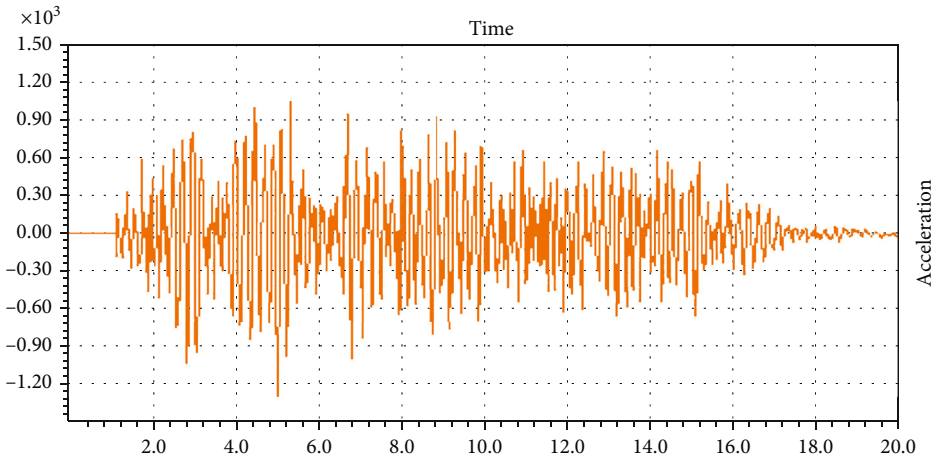

(b) Lanzhou seismic wave

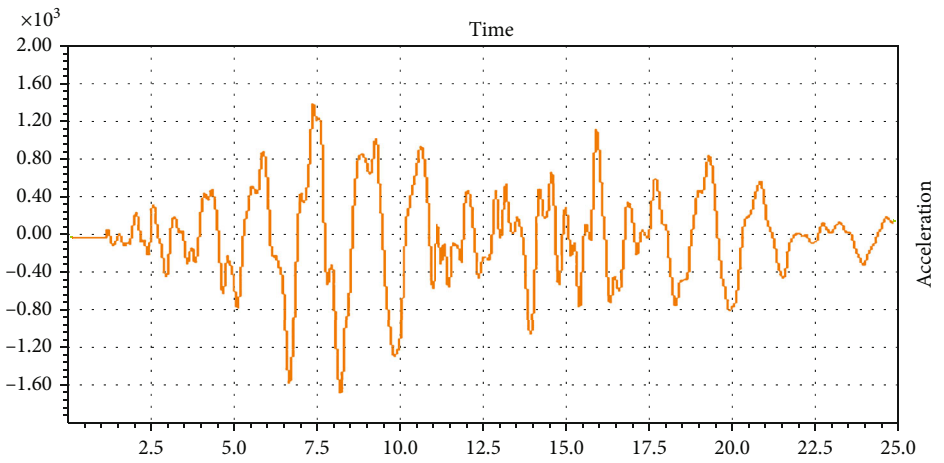

(c) Shanghai artificial seismic waves

Figure 4: Seismic wave waveform.

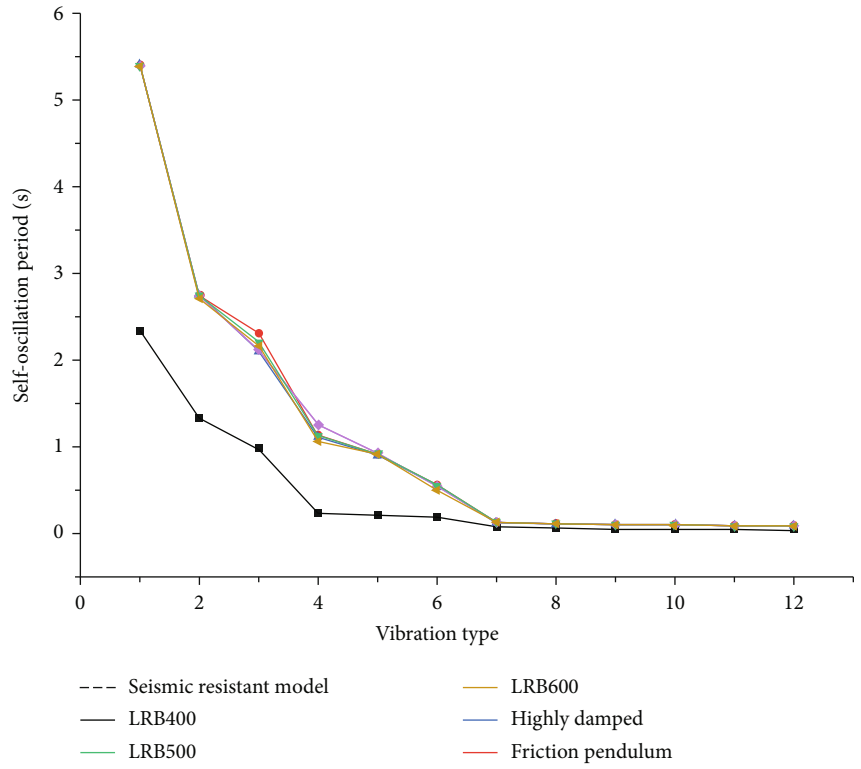

Figure 5: Periodic comparison between the original structure and the five types of seismic isolation structures.

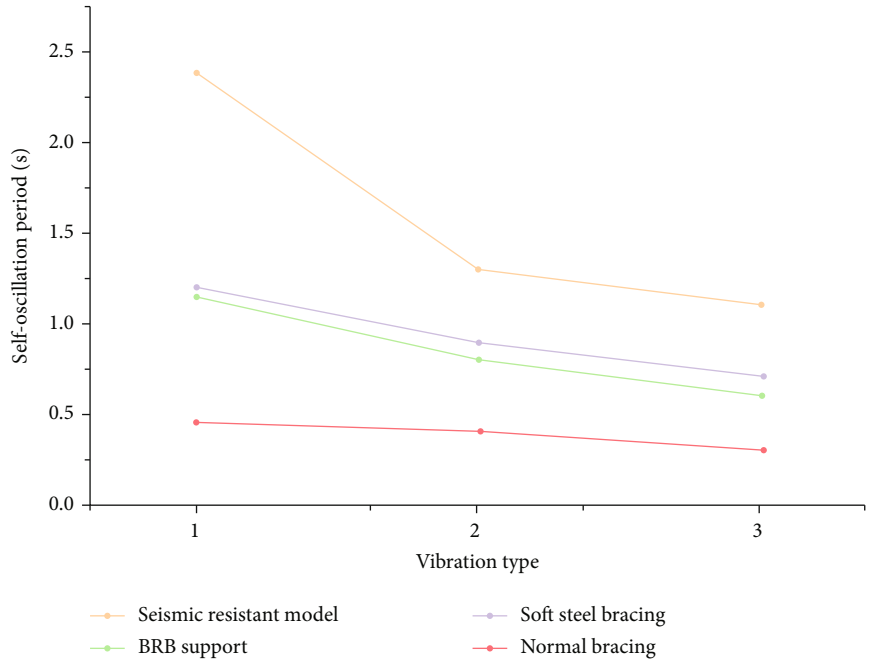

Figure 6: Periodic comparison between the seismic-resistant model and the three types of seismic-damped models.

diagram of the top displacement of the structure in Figure 8, the top displacement of the five types of structures incorporating seismic isolation bearings and the three types of structures with bracing are all smaller than the seismic-resistant model under the three waves. The vertex displacement curves of LTB400, LTB500, and LTB600 in the seismic-isolated system almost overlap and are smaller than the vertex displacements generated by high damped and friction

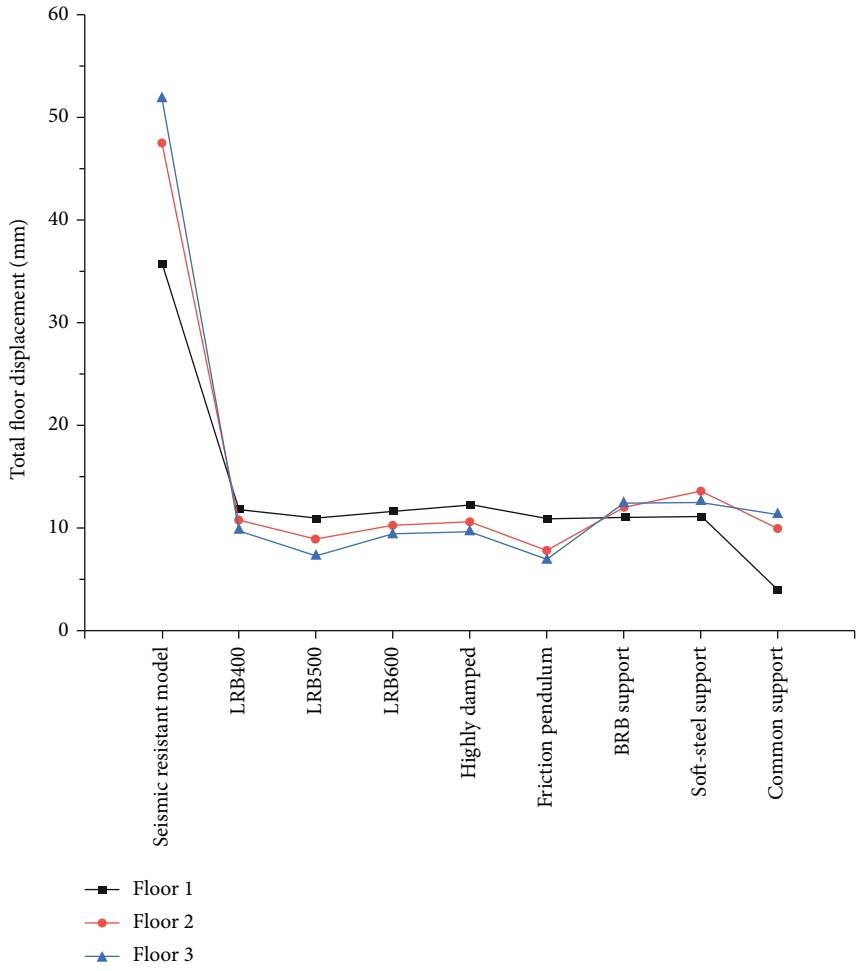

(a) EL-Centro wave

Figure 7: Continued.

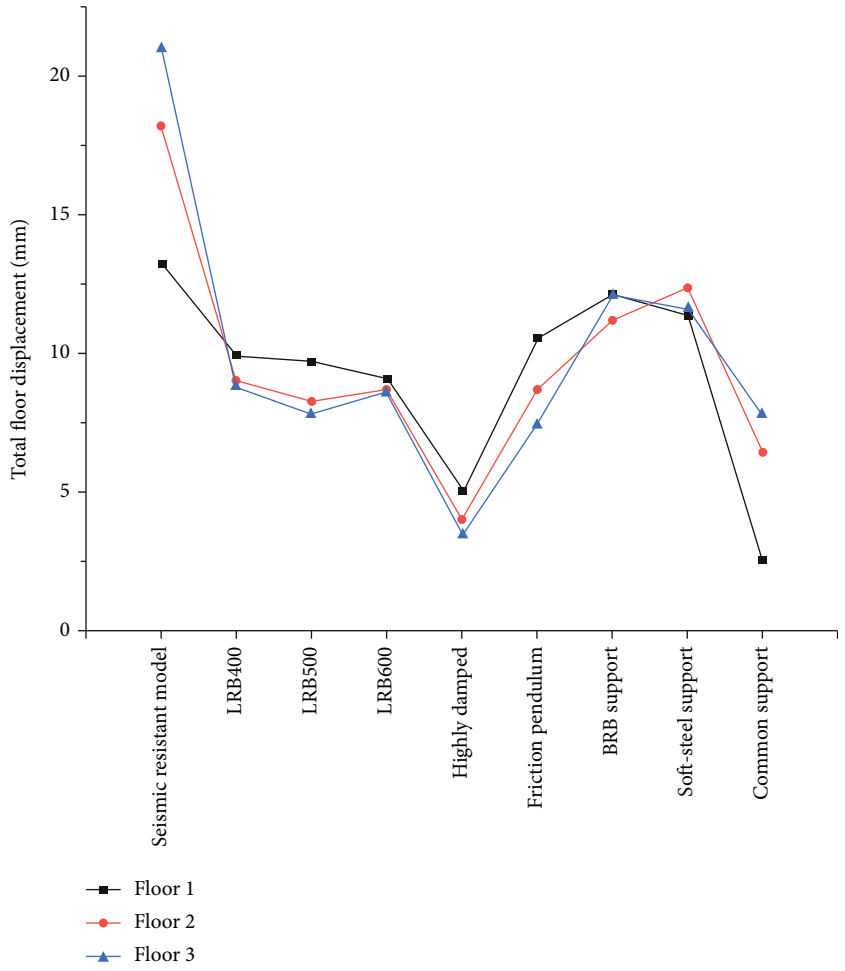

(b) Lanzhou wave

Figure 7: Continued.

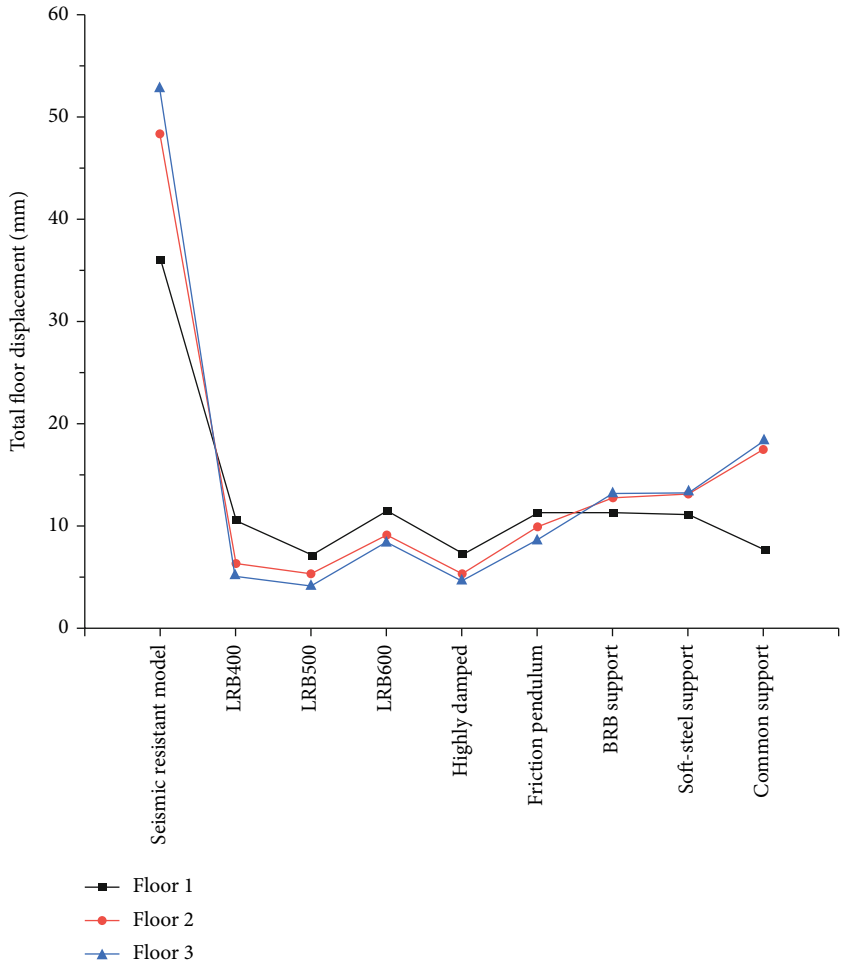

(c) Shanghai artificial wave

Figure 7: Comparison of total displacement of floors of various systems under different seismic waves.

pendulum; the vertex displacements of ordinary supports in the damped system are smaller than those of soft-steel supports and BRB supports.

4.2. Comparison of Base Shear. A comparison of the basal shear is shown in Table 3, and the data indicates the following:

(1) There are some differences in foundation shear values under different seismic waves. The seismic-resistant model has the highest shear values under the action of all three seismic waves

(2) The foundation shear of the five options of the seismic-isolated models is substantially reduced under seismic action. Under the EL-Centro wave, the foundation shear values are as follows: high damped<friction pendulum<LRB600<LRB400<LRB500. Under the Lanzhou wave, the foundation shear values are as follows: high damped<friction pendulum<LRB400<LRB600<LRB500. Under the Shanghai artificial wave, the foundation shear values are as follows: friction pendulum<high damped<LRB600<LRB400<LRB500. The foundation shear values of the damped structure show such a relationship under the action of three kinds of seismic waves: BRB bracing<soft-steel bracing<normal bracing

(3) Comparing the foundation shear data for the five options of the seismic-isolated system and the three options of the seismic-damped system, the values for all five options of the seismic-isolated models are smaller than those for the seismic-damped models

4.2.1. Structural Acceleration Response. The vibration acceleration of the structure is one of the important parameters in analysing the response of the structure to seismic waves. Comparison of the acceleration of seismic-resistant model, seismic-isolated models and seismic-damped models are shown in Figure 9.

As can be seen from Figure 9, the acceleration effects produced by LTB400, LTB500, and LTB600 are close under the action of the three waves, and the acceleration effects under EL-Centro and Lanzhou waves are less than

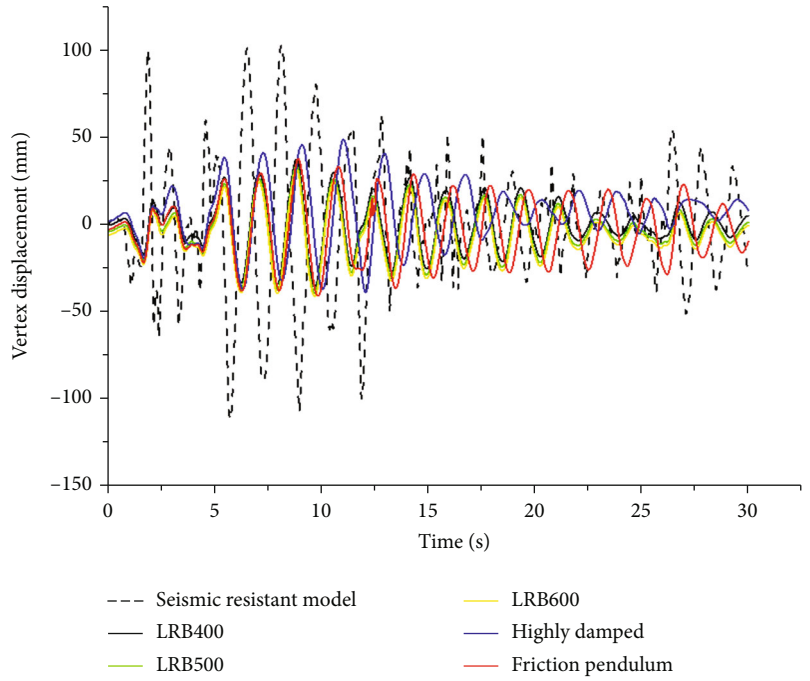

(a) Comparison of the vertex displacements of the seismic-resistant model and the seismic-isolated models under EL-Centro waves

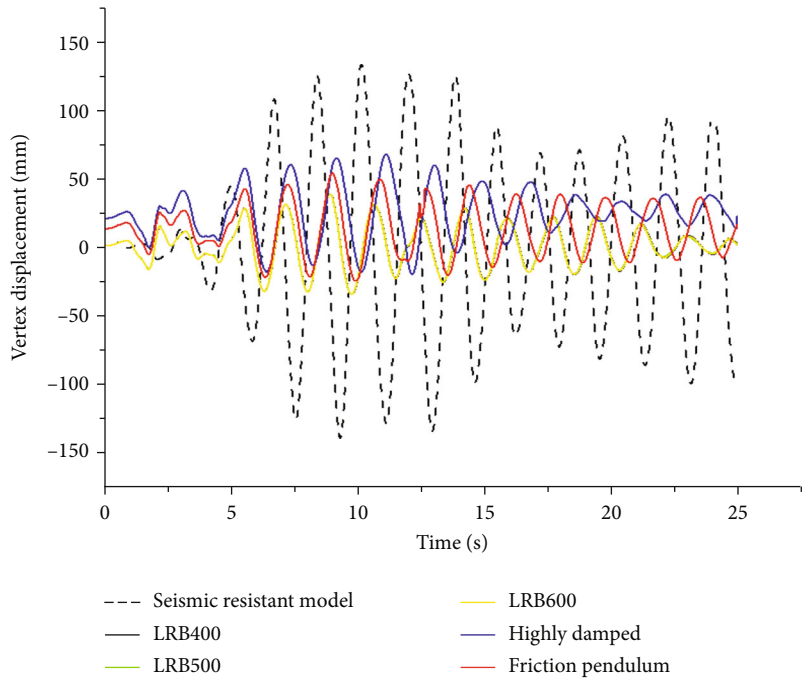

(b) Comparison of the vertex displacements of the seismic-resistant model and the seismic-isolated models under Shanghai artificial waves

Figure 8: Continued.

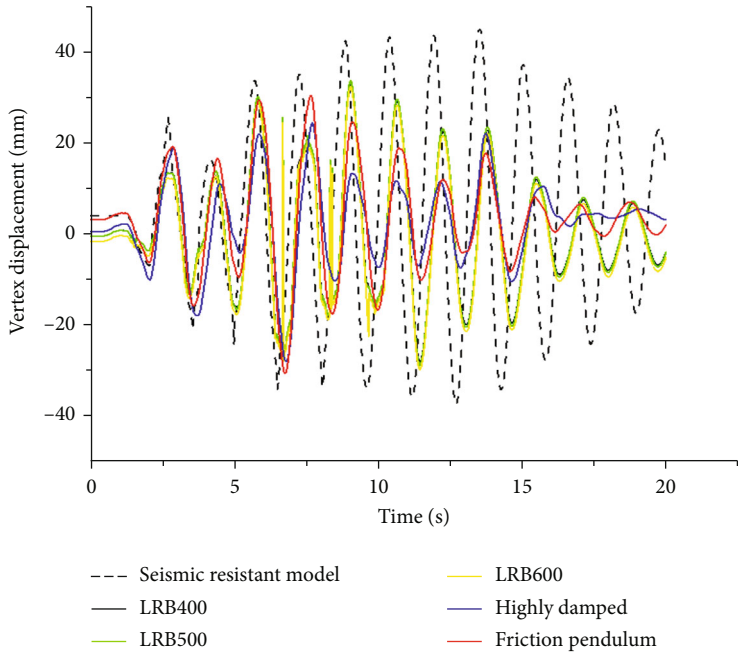

(c) Comparison of the vertex displacements of the seismic-resistant model and the seismic-isolated models under the Lanzhou wave

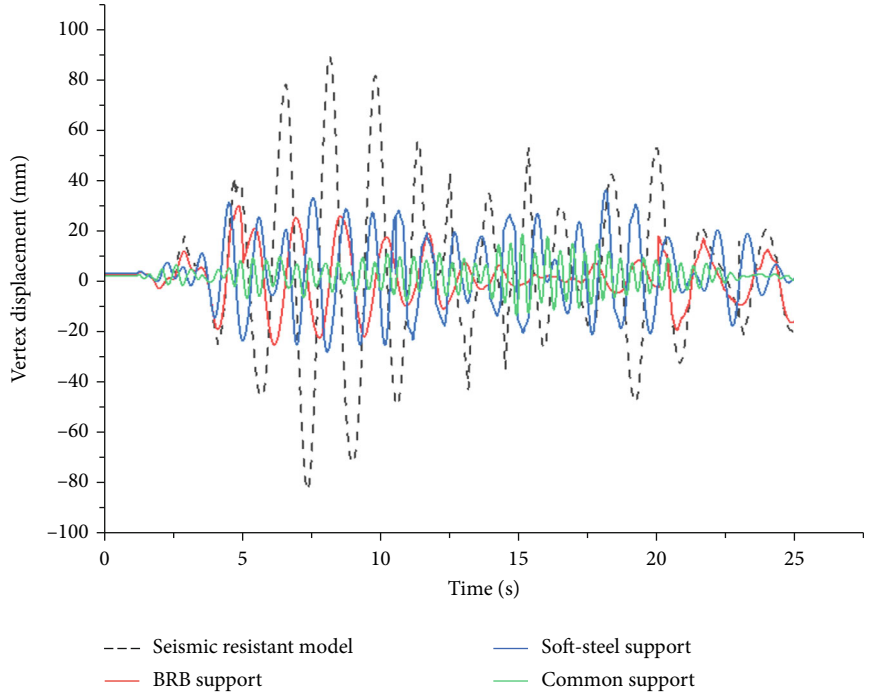

(d) Comparison of the vertex displacements of the seismic-resistant model and the seismic-damped models under EL-Centro waves

Figure 8: Continued.

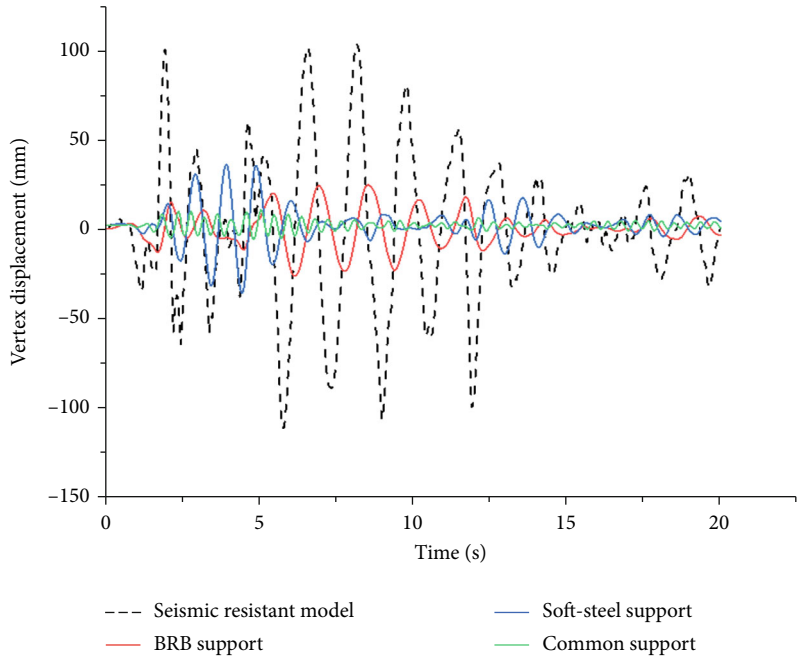

(e) Comparison of the vertex displacement of the seismic-resistant model and the seismic-damped models under Shanghai artificial waves

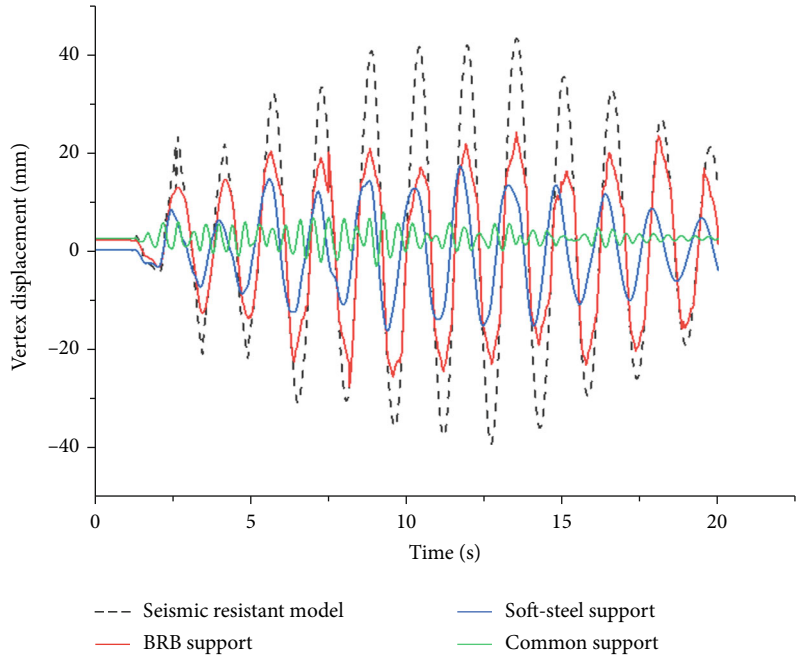

(f) Comparison of vertex displacements of the seismic-resistant model and the seismic-damped models under the Lanzhou wave

Figure 8: Time diagram of displacement at the apex of the structure.

those of the high damped and friction pendulum. The acceleration at the upper floors of the different seismic-isolated structures is substantially reduced compared to the seismic-resistant model.

5. Economic Performance Analysis

5.1. Introduction to Whole Life Cycle Costs. Jiang et al. [39] analysed the cost of resistance, seismic isolated, and seismic damped of buildings and compared the economic differences between the three.

The design life of a building is generally 50 years, and the following costs are generally incurred during the service life cycle: direct construction costs, including building construction, renovation, and the addition of various indoor equipment. Banerjee and Patro and Li et al. [33, 35] analysed the composition of the whole-life costs and established a widely used cost assessment model for the initial cost of foundation seismic-isolated structures, which suitable for

Table 3: Comparison of base shear force of each structure type under three seismic waves (unit: kN).

	Seismic waves		
	EL-Centro wave	Lanzhou wave	Shanghai artificial wave
Seismic-resistant model	130.12	152.62	208.6
Highly damped	84.52	54.02	63.72
Friction pendulum	96.3	77.78	54.64
LRB400	109.38	92.54	110.54
LRB500	109.78	93.98	112
LRB600	109	93.42	110.02
BRB support	118.16	143.42	190.26
Soft-steel support	123.34	144.7	197.2
Common support	127.3	149.32	203.06

both preliminary estimation and detailed calculation. The model gives the loss cost composition and calculation method based on the failure of the seismic-isolated structure.

5.1.1. Direct Construction Costs. Analysis from the perspective of direct construction economic costs: a survey of the existing seismic-isolated structures in China shows that the cost of seismic-isolated structures is related to the intensity of the area where they are located, the type of structure, and the number of storeys of the structure.

The seismic-isolated model increases the cost of seismic-isolated bearings, which increase the cost of the seismic-isolated layer, additional strengthening of basement columns, and the seismic-damped system in the floor is also an important part. With the addition of seismic-isolated design, the scope of foundation treatment can be reduced; the main structure can reduce the cross section of the main structure and connect nonstructural elements, simplifying and reducing the cost of the structure.

The design cost of seismic-isolated model will increase by 0.1%~0.5% due to the increase of seismic-isolated layers [40]. The initial direct construction cost C_1 [36] of the structure after the use of seismic isolated and damping measures is expressed as shown below.

$$\begin{aligned} C_1 &= C_S + C_{I-\mathrm{iso}} - C_{\mathrm{sd}}, \\ C_{I-\mathrm{iso}}(I_d) &= \beta(I_d) \times C_S, \end{aligned} \tag{1}$$

In the equation, C_s is the total initial cost of design and construction without seismic-isolated measures; $C_{I-\mathrm{iso}}$ is the increase in cost due to the use of seismic-isolated measures; C_{sd} is the reduction in seismic cost of the superstructure due to the use of seismic-isolated measures with reduced intensity design. The results of the literature [41] show that the average values of $\beta(I_d)$ are 6.2%, 8.5%, and 9.5% in the areas with 7, 8, and 9 degrees of seismic protection, respectively. $\alpha(I_d)$ is the value of the cost increase coefficient for seismic protection, and some statistics in China suggest that the increase in building cost is 3% to 8%, 10% to 15%, and 25% to 40% in VII, VIII, and IX degree areas, respectively.

Superstructure strength standards for earthquake-resistant or earthquake-isolated buildings can be appropriately lowered. At the same seismic intensity, the size of the beams and columns and the reinforcement of the superstructure are reduced by the use of seismic-damped technology, which reduces the cost compared to seismic-resistant buildings. The cost savings for the upper part of the building are calculated using the literature [37] for a seismic-isolated scheme without changing the structural type of the building C_{sd}:

$$C_{\mathrm{sd}}(I^*_d) = \gamma(I^*_d) \times C_0. \tag{2}$$

In the equation, $I*_d$ is the reduced intensity of the superstructure and $I*_d$ is the integer intensity, and then $\gamma(I*_d) = \alpha(I_d) - \alpha(I*_d)$. C_0 is the initial cost of the structure when seismic protection is not considered.

5.1.2. Inspection and Maintenance Costs. During the whole life cycle of the building structure, in order to ensure the safety of the use of the structure, the cost of inspecting and maintaining the building structure so that it can achieve its original use function. As antiageing materials are added to the seismic-isolated bearings and dampers, they are more slowly in daily use and their service life is generally longer than the life of the building.

5.1.3. Postearthquake Damage Costs. Analysed from a long-term perspective, the scenario of a building structure experiencing a larger earthquake is taken into account. The direct economic damage costs are the cost of the damage to the building itself, the loss of interior equipment, and furniture items; the indirect economic damage is the loss of economic benefit due to the loss of use of the building after the damage has occurred. The direct damage loss caused by earthquake mainly consists of two parts: acceleration and displacement caused by structure. The large displacements and accelerations of the structure can lead to the damage of the main load-bearing members and various internal equipment when a nonseismic damped or isolated building is affected by an earthquake. The deformation of the seismic-isolated system occurs in the seismic-isolated layer, and the upper structure will level the isolated layer, which will reduce

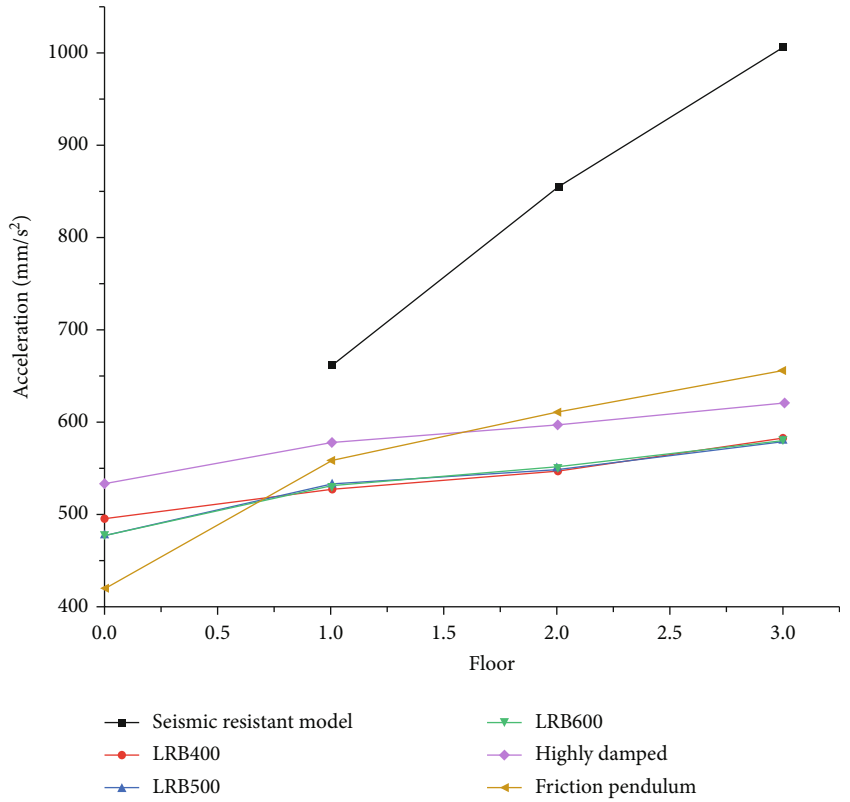

(a) EL-Centro wave

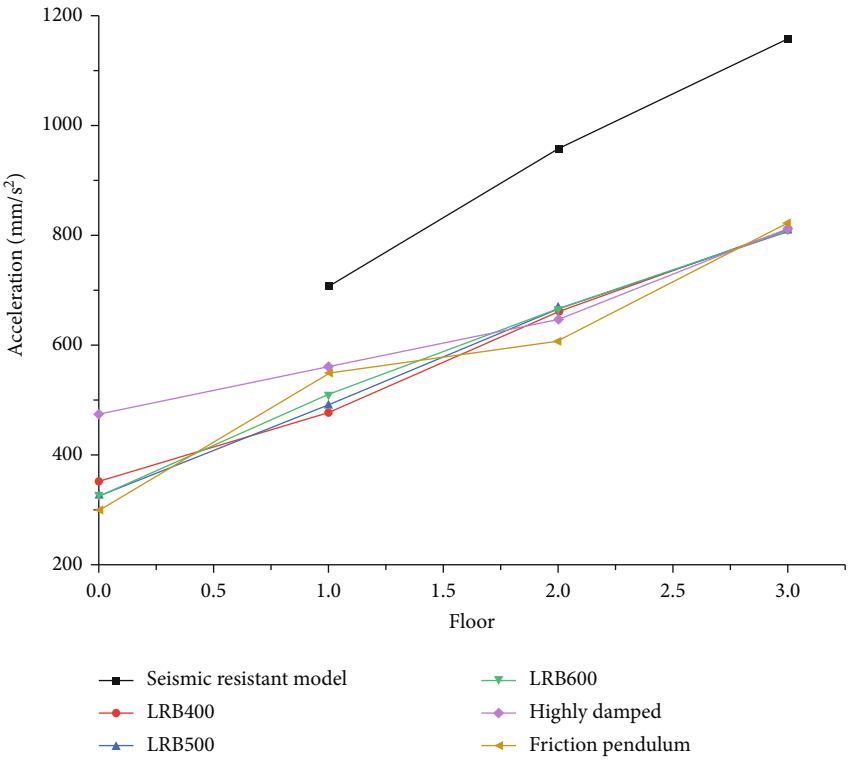

(b) Lanzhou wave

Figure 9: Continued.

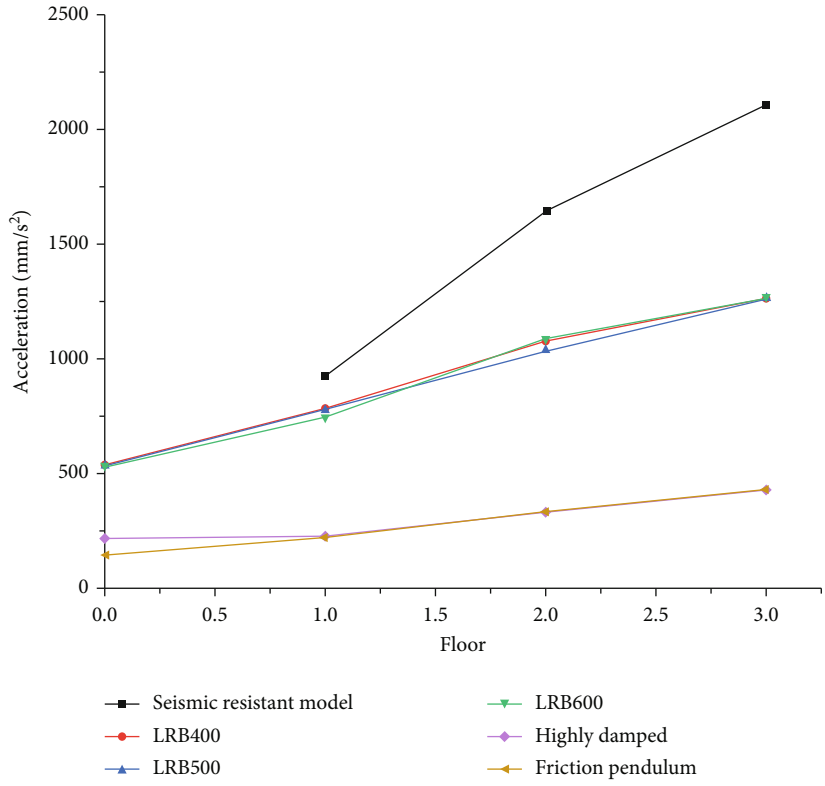

(c) Shanghai artificial wave

Figure 9: Comparison of floor acceleration between the seismic-resistant model and the seismic isolation models under seismic waves.

the seismic response compared to the seismic-resistant structure; the seismic-damped structure will provide lateral stiffness due to the effect of the damping dampers, which will prevent the building from displacement, and the seismic response caused by displacement will be less. As a result, seismic-isolated structures are much less costly than the seismic-resistant structure in terms of damage incurred during an earthquake and postearthquake repairs. This shows that the use of seismic-isolated techniques is thus effective in reducing direct economic losses. Kilar et al. [42] showed that seismic-isolated systems are effective in controlling damage costs under medium height earthquake effects.

5.2. Comparison of Economic Performance. This paper analyses an example of a light steel-wood-plastic structure project in Xishuangbanna, a 2-storey light steel-wood-plastic residence with a construction area of 172.2 m^2 and a structural intensity of 8 degrees. According to the market price of light steel estimated at 237.3$ per square metre, the price of wood-plastic estimated at 31.6$ per square metre, the actual construction of the original structure estimates the total cost of 47453.3$. Tables 4 and 5 show the current prices of seismic-isolated bearings and seismic dampers applicable to the building.

Table 4 shows that the initial cost of the structures with seismic-isolated bearings and seismic dampers increased compared to the seismic-resistant model with the percentage increase varying according to the price of the bearings and dampers. The five options in the seismic-isolated system increase the cost by 10.3%, 12.9%, 23.6%, 12.9%, and 16.9%, respectively, while the two structures in the seismic-damped system increase the cost by 11.3% and 9.6%, respectively.

Table 4: Isolation support price information.

Name	LRB400	LRB500	LRB600	High damping support	Friction pendulum
Price ($)	237.3	316.4	632.7	316.4	363.8

Table 5: Different damper price information.

Name	BRB supports	Flexible metal steel supports
Price ($)	1075.6	870.0

The economic analysis of seismic-isolated and seismic-damped structures is mainly based on the comparison of acquisition costs of isolation bearings and dampers. The number of seismic-isolated bearings used in this paper is 16, and the number of seismic dampers is 4.

As can be seen from Table 5, the inspection and maintenance costs of each support and damper have decreased relative to the seismic-resistant structure, with a decrease of 3.8 to 4.9%.

Table 6: Direct construction costs for each structure.

Name	Price ($)	Number (pcs)	Cost $C_{I-\mathrm{iso}}$ ($)	Total initial cost C_1 ($)	Increase compared to original structure ($)
LRB400	237.3	16	3798.7	52359.2	4875.0
LRB500	316.4	16	5065.0	53625.4	6141.3
LRB600	632.7	16	10130	58690.4	11206.3
Highly damped	316.4	16	5065.0	52359.2	6141.3
Friction pendulum	363.8	16	5824.7	55524.8	8040.6
BRB supports	1075.6	4	4305.2	52865.7	5381.5
Flexible metal steel supports	870.0	4	3482.2	52042.6	4558.5

5.2.1. Direct Construction Costs. The total direct construction cost of the structure directly using traditional seismic measures is $C_S = 47484.1\$$; due to the simplicity of the structure, the design fee for the seismic-isolated layer is taken as 0.1%, so the design fee increases by 47.5$. The initial construction cost corresponding to the reduction of the intensity of the upper structure after the adoption of seismic-damped and seismic-isolated technology is $C_{\mathrm{Sd}} = 3005.4\$$; the other costs of the structure cost increase by adopting seismic-damped and seismic-isolated measures are $C_{I-\mathrm{iso3}} = 4033.5\$$; the total initial cost of the seismic-damped and seismic-isolated structure is $C_1 = C_S + C_{I-\mathrm{iso1}} + C_{I-\mathrm{iso3}} + 0.03 - C_{\mathrm{sd}}$; the increased cost over the seismic-resistant structure is $C_1 - C_S$. The direct construction costs for each structure are shown in Table 6 below.

5.2.2. Inspection and Maintenance Costs. The maintenance cost of a seismic-resistant model is generally 2% of the initial cost; then, the seismic-resistant model inspection and maintenance cost is $C_M = C_S \times 2\% = 949.7\$$. Seismic-isolated and seismic-damped models take into account the increased safety factor of the superstructure, and the structural damage will be much smaller. This paper takes 1% of the initial cost, and the inspection and maintenance fees for each structure are shown in Table 7.

5.2.3. Postearthquake Losses. To simplify this part of the calculation, the total loss ratios of the seismic-isolated models and the seismic-resistant model are taken as 2.7% and 18.1%, respectively, in this paper [31]. And the loss ratios of seismic-damped models are taken as 5.9% [31]. Assuming that the total value of the building's interior property is equal to the total cost of the building structure itself, the seismic-resistant model loss value is as follows: $C_L = C_S \times 18.1\% = 8594.6\$$, and the postearthquake loss values for each structure in the seismic-isolated and seismic-damped systems are shown in Table 8 below.

The structural damage to the seismic-resistant structure is more severe under a large earthquake, resulting in a larger proportion of damage to the building structure and internal installations. The postearthquake loss values for each structure are calculated in Table 8 based on the proportion of losses under the earthquake for the seismic-isolated and seismic-damped systems. The post-earthquake loss costs are reduced by 82% to 84% for the seismic-isolated system compared to the seismic-resistant model, 64% for the seismic-damped system compared to the seismic-resistant model, and 49% to 55% for the seismic-isolated models compared to the seismic-damped models.

Table 7: Inspection and maintenance fees for each structure.

Name	Total initial cost C_1 ($)	Inspection and maintenance costs C_M ($)
LRB400	237.3	2.373
LRB500	316.4	3.164
LRB600	632.7	6.327
Highly damped	316.4	3.164
Friction pendulum	363.8	3.638
BRB supports	1075.6	10.756
Flexible metal steel supports	870.0	8.700

5.3. Whole Life Cycle Costs. As can be seen from the data in Table 9, the 600 mm diameter lead-core rubber bearing and friction pendulum selected are higher than the total cost incurred by the seismic-resistant structure. Considering that the three-story low-cost housing is cost limited, these two types of bearings are not suitable for expensive. Therefore, on the condition that the seismic-isolated effect is equally satisfied, the selection is made according to the advantages. The whole-life cost of the 400 mm, 500 mm, and high damping bearings for the seismic-isolated model was reduced by 2738.3$ and 1424.5$ compared to the seismic-resistant structure, resulting in a total cost reduction of 4.8% and 2.5% compared to the seismic-resistant model; the BRB support structure and the flexible metal steel support structure were reduced by 522.3$ and 1392.9$, respectively, resulting in a total cost reduction of 0.92% and 2.4% compared to the seismic-resistant model; The total cost of the vibration seismic-isolated system is 0.6%~3.9% lower than the total cost of the seismic-damped system.

Table 8: Postearthquake loss of each structure.

Name	Total initial cost C_1 ($)	Percentage of loss (%)	Postearthquake damage value C_L ($)
LRB400	237.3	2 .7	1413.4
LRB500	316.4	2.7	1448.3
LRB600	632.7	2.7	1582.8
Highly damped	316.4	2.7	1448.3
Friction pendulum	363.8	2.7	1503.7
BRB supports	1075.6	5.9	3118.1
Flexible metal steel supports	870.0	5.9.	3070.6

Table 9: Life cycle cost of each structure.

Name	Whole life cycle cost $C = C_S + C_M + C_L$ ($)	Difference to original structure cost ($)
Seismic-resistant model	47484.1 + 949.7 + 8594.6 = 57028.4	/
LRB400	52359.2 + 523.592 + 1413.4 = 54296.2	-2738.3
LRB500	53625.4 + 536.254 + 1448.3 = 55610.0	-1424.5
LRB600	58690.4 + 586.904 + 1582.8 = 60858.8	+3830.4
Highly damped	53625.4 + 536.254 + 1448.3 = 55610.0	-1424.5
Friction pendulum	55524.8 + 555.248 + 1503.7 = 57582.4	+554.0
BRB supports	52865.7 + 528.657 + 3118.1 = 56506.1	-522.3
Flexible metal steel supports	52042.6 + 520.426 + 3070.6 = 55635.6	-1392.9

6. Conclusion

This paper uses the SAP2000 finite element software to study the nonlinear time history analysis of the seismic model, isolation model, and shock absorption model of the new rural light steel-wood-plastic residential structure in Yunnan under the action of an 8-degree earthquake. The conclusions are summarized as follows:

(1) *Comparison of Vibration Periods of Light Steel-Wood-Plastic Structure*: LRB400>LRB600>friction pendulum>high damped≈LRB500>seismic-resistant model>BRB bracing>soft-steel bracing>ordinary bracing. The period of the seismic-isolated structure effectively avoids the excellent period of the site and reduces the seismic response of the seismic wave input to the structure

(2) As seen from the structural interstorey displacement, foundation shear, and acceleration diagrams, the values of LRB400, LRB500, and LRB600 are similar in the seismic-isolated system, and the values of friction pendulum and high damped differ from LRB400, LRB500, and LRB600, but the values are all smaller than those produced by the seismic-resistant model and seismic-damped models

(3) In terms of total force, the seismic-isolated models<the seismic-damped models<the seismic-resistant model, and the effect of using the seismic-isolated models are better than that of the seismic-damped models

(4) In terms of postearthquake damage costs, the total cost of the seismic-isolated models is 82%~84% lower than that of the seismic-resistant model, the total cost of the seismic-damped models is 64% lower than that of the seismic-resistant model, and the total cost of the seismic-isolated models is 49%~55% lower than that of the seismic-damped models. In terms of total life cycle costs, the total cost of the seismic-isolated models is 4.8% and 2.5% lower than that of the seismic-resistant model, and the total cost of the seismic-damped models is 0.92% and 2.4% lower than that of the seismic-resistant model. The total cost of the seismic-isolated models is 0.92% and 2.4% lower than that of the seismic-resistant model, and the total cost of the seismic-isolated models is 0.6% to 3.9% lower than the total cost of the seismic-damped models

In summary, the safety and economy of seismic-isolated models are superior to seismic-damped models. It can provide a reference for the promotion of seismic-isolated models in seismic zones. At the same time, the advantages of light steel-wood-plastic structures in terms of green ecology can provide some experience for the sustainable development of buildings.

Data Availability

All data included in this study are available upon request by contacting with the corresponding author.

Conflicts of Interest

The authors declare that there is no conflict of interests regarding the publication of this paper.

Authors' Contributions

The corresponding author is Dewen Liu, and the email address is civil_liudewen@sina.com.

Acknowledgments

No funds were received.

References

[1] Y. S. Tian, J. Wang, T. J. Lu, and C. Y. Barlow, "An experimental study on the axial behavior of coldformed steel wall studs and panels," *Thin-Walled Structure*, vol. 42, no. 4, pp. 557–573, 2004.

[2] P. Fredezc, *Miller Wood-plastic composite*, VDM Verlag Dr.Muellere.k, 2010.

[3] M. Nakashima, C. W. Roeder, and Y. Maruoka, "Steel moment frames for earthquakes in United Statesand Japan," *Journalof Structural Engineering*, vol. 126, no. 8, pp. 861–868, 2000.

[4] L. Yalin, *The Practice and Application of Low-Rise Cold-Formed Thin-Walled Light Steel Structure System in Post-Disaster Reconstruction*, Xi'an University of Architecture and Technology, 2011.

[5] M. Zhu, *Application of Cold-Formed Thin-Walled Steel Structure System in Low-Rise Industrialized Housing*, South China University of Technology, 2013.

[6] X. L. Li, Z. Y. Cao, and Y. L. Xu, "Characteristics and trends of coal mine safety development," in *Energy Sources, Part A: Recovery, Utilization, and Environmental Effects*, pp. 1–14, Taylor & Francis, 2020.

[7] C. Hongtao, *Simulated Seismic Shaking Table Tests on Multi-Storey Light Steel Keel Houses*, Nanjing University of Technology, 2008.

[8] P. Pan, L. P. Ye, W. Shi, and H. Y. Cao, "Engineering practice of seismic isolation and energy dissipation structures in China," *Science*, vol. 55, no. 11, pp. 3036–3046, 2012.

[9] H. Wu, G. Zhao, and S. Ma, "Failure behavior of horseshoe-shaped tunnel in hard rock under high stress: phenomenon and mechanisms," *Transactions of Nonferrous Metals Society of China*, vol. 32, no. 2, pp. 639–656, 2022.

[10] J. Ma, X. L. Li, J. G. Wang et al., "Experimental study on vibration reduction technology of hole-by-hole presplitting blasting," *Geofluids*, vol. 2021, Article ID 5403969, 10 pages, 2021.

[11] F. Zhou and P. Tan, "Recent progress and application on seismic isolation energy dissipation and control for structures in China," *Earthquake Engineering and Engineering Vibration*, vol. 17, no. 1, pp. 19–27, 2018.

[12] J. Wang, T. Zuo, X. Li, Z. Tao, and J. Ma, "Study on the fractal characteristics of the pomegranate biotite schist under impact loading," *Geofluids*, vol. 2021, Article ID 1570160, 8 pages, 2021.

[13] H. Zhu, Z. Fangyuan, and Y. Chong, "Research progress and analysis of seismic isolation structures in buildings," *Engineering Mechanics*, vol. 31, no. 3, pp. 1–10, 2014.

[14] Z. Fulin, "Seismic isolation, energy dissipation and damping and structural control system - an inevitable technical choice to terminate earthquake disasters in China's urban and rural areas," *Cities and Disaster Mitigation*, vol. 5, pp. 1–10, 2016.

[15] J. Yulong, *Research on Seismic Analysis and Seismic Isolation of Container Bank Bridge Structur*, Shanghai Jiaotong University, 2012.

[16] K. Yuan, J. Zhang, J. Guo, and W. Tian, "Study on seismic response characteristics and design parameters of composite isolation system for rural buildings," *KSCE Journal of Civil Engineering*, vol. 23, no. 4, pp. 1747–1755, 2019.

[17] X. G. Kong, D. He, X. F. Liu et al., "Strain characteristics and energy dissipation laws of gas-bearing coal during impact fracture process," *Energy*, vol. 242, p. 123028, 2022.

[18] X. G. Kong, S. G. Li, E. Y. Wang et al., "Experimental and numerical investigations on dynamic mechanical responses and failure process of gas-bearing coal under impact load," *Soil Dynamics and Earthquake Engineering*, vol. 142, p. 106579, 2021.

[19] W. Shen, S. Guocang, Y. Wang, B. Jianbiao, Z. Ruifeng, and X. Wang, "Tomography of the dynamic stress coefficient for stress wave prediction in sedimentary rock layer under the mining additional stress," *International Journal of Mining Science and Technology*, vol. 31, no. 4, pp. 653–663, 2021.

[20] Z. Li, X. Zhang, Y. Wei, and M. Ali, "Experimental study of electric potential response characteristics of different lithological samples subject to uniaxial loading," *Rock Mechanics and Rock Engineering*, vol. 54, no. 1, pp. 397–408, 2021.

[21] J. Z. Zhang, H. W. Huang, D. M. Zhang, M. L. Zhou, C. Tang, and D. J. Liu, "Effect of ground surface surcharge on deformational performance of tunnel in spatially variable soil," *Computers and Geotechnics*, vol. 136, article 104229, 2021.

[22] L. Li, H. Liu, W. Wu, M. Wen, M. H. El Naggar, and Y. Yang, "Investigation on the behavior of hybrid pile foundation and its surrounding soil during cyclic lateral loading," *Ocean Engineering*, vol. 240, article 110006, 2021.

[23] A. Natale, C. Del Vecchio, and M. Di Ludovico, "Seismic retrofit solutions using base isolation for existing RC buildings:economic feasibilty and pay-back time," *Bulletin of Earthquake Engineering*, vol. 19, no. 1, pp. 483–512, 2021.

[24] A. V. Favorskaya and I. B. Petrov, "Study of seismic isolation by full-wave numerical modeling," *Doklady Earth Sciences*, vol. 481, no. 2, pp. 1070–1072, 2018.

[25] A. Li, "Vibration Control Engineering Practice for the Multi-story and Tall Building Structure," in *Vibration Control for Building Structures*, Springer Tracts in Civil Engineering., Springer, Cham, 2020.

[26] T. Wang, *Seismic Response Analysis and Seismic Damping Techniques for Large-Span Cable-Stayed Bridges*, Tongji University, 2007.

[27] L. Xuanmin, *Application of Friction Pendulum System in Seismic Strengthening of Frame Structure*, Beijing Jiaotong University, Beijing, 2014.

[28] Z. H. O. U. Ying, H. U. Chengcheng, and Z. H. O. U. Guangxin, "Research on the design method of shaking table model for friction pendulum isolation structure," *Structural Engineer*, vol. 5, pp. 6–11, 2015.

[29] Y. Nakamura and K. Okada, "Review on seismic isolation and response control methods of buildings in Japan," *Geoenvironmental Disasters*, vol. 6, no. 1, 2019.

[30] L. Di Sarno, E. Chioccarelli, and E. Cosenza, "Seismic response analysis of an irregular base isolated building," *Bulletin of Earthquake Engineering*, vol. 9, no. 5, pp. 1673–1702, 2011.

[31] B. Shahbazi and E. Moaddab, "A new hybrid friction damper (HFD) for dual-level performance of steel structures," *International Journal of Streel Structures*, vol. 21, no. 4, pp. 1332–1345, 2021.

[32] B. Dong, R. Sause, and J. M. Ricles, "Modeling of nonlinear viscous damper response for analysis and design of earthquake-resistant building structures," *Bulletin of Earthquake Engineering*, vol. 20, no. 3, pp. 1841–1864, 2022.

[33] S. Banerjee and S. K. Patro, "Inelastic seismic response of building with friction damper," *Journal of The Institution of Engineers (India): Series A*, vol. 97, no. 4, pp. 395–404, 2016.

[34] A. H. Deringöl and E. M. Güneyisi, "Effect of Using High Damping Rubber Bearings for Seismic Isolation of the Buildings," *International Journal of Steel Structures*, vol. 21, no. 5, pp. 1698–1722, 2021.

[35] X. L. Li, S. J. Chen, S. M. Liu, and Z. H. Li, "AE waveform characteristics of rock mass under uniaxial loading based on Hilbert-Huang transform," *Journal of Central South University*, vol. 28, no. 6, p. 2021, 2021.

[36] S. Liu, X. Li, D. Wang, and D. Zhang, "Experimental study on temperature response of different ranks of coal to liquid nitrogen soaking," *Natural Resources Research*, vol. 30, no. 2, pp. 1467–1480, 2021.

[37] J. Z. Zhang, K. K. Phoon, D. M. Zhang, H. W. Huang, and C. Tang, "Novel approach to estimate vertical scale of fluctuation based on CPT data using convolutional neural networks," *Engineering Geology*, vol. 294, p. 106342, 2021.

[38] M. He, Z. Q. Zhang, J. W. Zhu, N. Li, G. Li, and Y. S. Chen, "Correlation between the rockburst proneness and friction characteristics of rock materials and a new method for rockburst proneness prediction: field demonstration," *Journal of Petroleum Science and Engineering*, vol. 205, article 108997, 2021.

[39] J. Shujiang, Y. Shunzhong, and L. Dewen, "Economic performance analysis of seismic isolation, energy dissipation, and traditional seismic structures," *E3S Web of Conferences*, vol. 248, article 01032, 2021.

[40] Y. Ma, Z. Guifeng, and P. Tan, "Study on the whole-life cost of seismically isolated structures," *Earthquake Engineering and Engineering Vibration*, vol. 32, no. 5, pp. 178–185, 2012.

[41] L. Zengxin and Y. Dong, *Economic Analysis of Seismically Isolated Frame Structures*, Engineering Construction and Design, 2014.

[42] V. Kilar, S. Petrovčič, D. Koren, and S. Šilih, "Cost viability of a base isolation system for the seismic protection of a steel high-rack structure," *International Journal of Streel Structures*, vol. 13, no. 2, pp. 253–263, 2013.